coatings

MDPI

Article

Development of Antibacterial Composite Films Based on Isotactic Polypropylene and Coated ZnO Particles for Active Food Packaging

Clara Silvestre [1,*], Donatella Duraccio [2], Antonella Marra [1], Valentina Strongone [1] and Sossio Cimmino [1]

Received: 11 December 2015; Accepted: 15 January 2016; Published: 22 January 2016
Academic Editor: Stefano Farris

[1] Institute of Polymers, Composites and Biomaterials, Consiglio Nazionale delle Ricerche (IPCB/CNR) Via Campi Flegrei 34, Naples 80078, Italy; antonella.marra@ipcb.cnr.it (A.M.); valentina.strongone@outlook.it (V.S.); sossio.cimmino@cnr.it (S.C.)
[2] Istituto per le Macchine Agricole e Movimento Terra, Consiglio Nazionale delle Ricerche (IMAMOTER-CNR) Strada delle Cacce 73, Torino 10135, Italy; donatella.duraccio@cnr.it
* Correspondence: clara.silvestre@cnr.it; Tel.: +39-081-867-5067; Fax: +39-081-867-5230

Abstract: This study was aimed at developing new films based on isotactic polypropylene (iPP) for food packaging applications using zinc oxide (ZnO) with submicron dimension particles obtained by spray pyrolysis. To improve compatibility with iPP, the ZnO particles were coated with stearic acid (ZnOc). Composites based on iPP with 2 wt % and 5 wt % of ZnOc were prepared in a twin-screw extruder and then filmed by a calender. The effect of ZnOc on the properties of iPP were assessed and compared with those obtained in previous study on iPP/ZnO and iPP/iPPgMA/ZnO. For all composites, a homogeneous distribution and dispersion of ZnOc was obtained indicating that the coating with stearic acid of the ZnO particles reduces the surface polarity mismatch between iPP and ZnO. The iPP/ZnOc composite films have relevant antibacterial properties with respect to *E. coli*, higher thermal stability and improved mechanical and impact properties than the pure polymer and the composites iPP/ZnO and iPP/iPP-g-MA/ZnO. This study demonstrated that iPP/ZnOc films are suitable materials for potential application in the active packaging field.

Keywords: isotactic polypropylene; zinc oxide; properties; active packaging; composites

1. Introduction

It is extensively reported that the nano/microparticles of zinc oxide (ZnO) exhibit antibacterial activity against gram-positive and gram-negative bacteria. This activity does not require the presence of UV light (unlike TiO_2), being stimulated by visible light, and it is inversely dependent on particle size [1–5]. The mechanisms responsible for the antibacterial activity are not fully understood. Distinctive mechanisms that have been put forward in the literature are listed as the following: direct contact of ZnO with cell walls, resulting in destructing bacterial cell integrity [6–8], liberation of antimicrobial ions, mainly Zn^{2+} ions [8], and reactive oxygen species formation [9–11].

There has been a great deal of interest in the antimicrobial property of ZnO for food packaging applications, as a viable solution for stopping infectious diseases [12–14]. Due also to low cost, ZnO particles (with sub-micro and nano-dimensions) are therefore ideal fillers for polymers to be applied in the field of active food packaging. Thus, ZnO particles have been incorporated into a number of different polymers used in food packaging [15,16], such as low-density polyethylene (LDPE) [17,18], isotactic polypropylene (iPP) [19–24], polyamide (PA) [18,25], and polylactic acid (PLA) [26].

Recently, the influence of ZnO particles, obtained by spray pyrolysis with submicron dimensions [22,27,28], on the structure, morphology, thermal stability, photo stability, and mechanical and antibacterial properties of (iPP)/ZnO composites was investigated [22,24]. The addition of ZnO particles imparts improvements on the photodegradation resistance of iPP to ultraviolet irradiation and the composites exhibit significant antibacterial activity against *Escherichia coli*. This activity is dependent on exposure time and composition.

On the other hand, it was noticed that due to the surface polarity mismatch between iPP and ZnO, agglomeration phenomena of the ZnO particles occur and that these phenomena cause a decrease in the mechanical and other functional properties of iPP/ZnO composites with respect to plain iPP [22–24].

The main problem to be solved in adding ZnO nano/microparticles to an iPP matrix seems therefore related to the formation of agglomerated domains that occur because of the strong intermolecular interactions among the ZnO particles in combination with their high surface area. This prevents transfer of their superior properties to the composite. Good dispersion has been reported for some polar polymers [18,25], but ZnO dispersion in non-polar polymers, such as iPP, during melt processing remains a challenge.

A largely proposed strategy, to improve dispersion consists in adding a compatibiliser, containing groups suitable for interaction with the two components [29–33]. Following this strategy in a previous paper, polypropylene grafted with maleic anhydride (PPgMA) [24] was selected as the most promising candidate as a compatibiliser between iPP and ZnO. In particular, the influence of three PPgMA (with different MW and MA% content) added to iPP/ZnO 98/2 wt % on the structure, morphology, mechanical, thermal, barrier properties and antibacterial activity against *E. coli* was investigated with the aim to verify if the compatibiliser PPgMA could be beneficial in order to increase the dispersion of ZnO in an iPP matrix in order to have films with improved properties. It was found that the presence of this compatilizer improves the dispersion of the particles in the matrix, but, at the same time, does not cause any enhancement in the barrier and mechanical properties and indeed reduces the antibacterial activity with respect to iPP/ZnO. An important aspect found in this study is that the more the ZnO are well embedded in polymer material, the more the antibacterial activity decreases, probably because the surface of the particle available for contact with the solution decreases.

An alternative methodology to improve the dispersion consists of modifying the particles' surfaces with groups suitable for interaction with the matrix.

The main purpose of this paper is to develop new films based on iPP for applications in the food industry as active packaging using coated ZnO particles to improve compatibility between the organic phase and inorganic one. In particular, the surface of the ZnO particles, obtained by spray pyrolysis, was coated with stearic acid (ZnOc). Objective of the paper is also to assess the influence of the coating process on the structure, morphology, and thermal stability of the zinc oxide particles.

2. Experimental

2.1. Materials and Sample Preparation

The materials used in this work are: (1) isotactic polypropylene (iPP, Moplen X30S), in pellets, kindly supplied by Basell (Ferrara, Italy), with melt flow index = 9 dg·min^{-1} (2.16 kg, 230 °C), $M_w = 3.5 \times 10^5$ and $M_n = 4.7 \times 10^4$; (2) zinc oxide coated with stearic acid (ZnOc) (white powder). The ZnO particles were synthesized using a preindustrial spray scale pyrolysis platform at the Pylote in Toulouse-France and then coated with stearic acid. This technique [22,27,28] provides many advantages compared to other techniques of preparation: the simplicity of the process, high purity of the powders obtained, more uniform chemical composition, narrow size distribution, better regularity in shape and the ability to synthesize multicomponent materials. The coating of the ZnO particles was performed by preparing a solution of stearic acid and ZnO (1:10) in isopropanol under stirring for 12 h. The powder was recovered by centrifuge and dried in an oven at a temperature of 70 °C.

2.2. Composite Preparation

The powders of ZnOc were mixed with iPP at two different compositions: 2% and 5% (see Table 1), in a twin screw extruder Collin ZK 25 (D = 25 mm and L/D = 24).

Table 1. Isotactic polypropylene/Zinc oxide coated with stearic acid (iPP/ZnOc) mixtures.

Sample	iPP (wt %)	ZnOc (wt %)
iPP	100	–
iPP/2%ZnOc	98	2
iPP/5%ZnOc	95	5

The temperature setting of the extruder from the hopper to the die was: 180/195/195/190/180 °C. The screw speed of the dispenser was 20 rpm while the speed of the extruder screws was 25 rpm.

Films of iPP and iPP/ZnOc were obtained by compression molding in a press at 210 °C and 100 bars. The films had a thickness of about 110–120 μm.

2.3. Characterization

The following technologies were used to determine the properties of the films:

1) FT-IR Spectroscopy

Infrared spectra of the compression molded films were recorded with a PerkinElmer FT-IR spectrometer, model Paragon 500 equipment (PerkinElmer, Boston, MA, USA). The IR spectra were recorded in the range 4000–800 cm^{-1} with 4 cm^{-1} resolution and 20 scans.

2) Wide-Angle X-ray Diffraction

Wide-angle X-ray diffraction (WAXD) measurements were conducted using a Philips XPW diffractometer (Philips, Almelo, The Netherlands) with CuKa radiation (1.542 Å) filtered by nickel. The scanning rate was 0.02°/s and the scanning angle was from 5° to 45°. The ratio of the area under the crystalline peaks and the total area multiplied by 100 was taken as the crystalline percentage degree.

3) Thermogravimetric Analysis

The thermal stability of the blends was examined by thermogravimetric analysis (TGA), using a PerkinElmer-Pyris Diamond apparatus (PerkinElmer, Boston, MA, USA) with a heating rate of 10 °C/min in air. Two measurements were performed for each sample.

4) Scanning Electron Microscopy

The surface analysis was performed using SEM, Fei Quanta 200 FEG (Fei, Hillsboro, OR, USA), on particles of the powders and on cryogenically fractured surfaces of composites. Before the observation, samples were coated with an Au/Pd alloy using an E5 150 SEM coating unit.

5) Tensile Tests

Dumbbell-shaped specimens were cut from the compression molded films and used for the tensile measurements. Stress–strain curves were obtained using an Instron machine, Model 4505 (Instron, Torino, Italy) at room temperature (25 °C) at a crosshead speed of 5 mm/min. Ten tests were performed for each composition.

6) Charpy Impact Test

The impact test allows for determining the degree of toughness of a polymer. Charpy impact tests were performed by using a pendulum CEAST (CEAST, Torino, Italy) with appropriate software for processing the data. The tests were carried out at room temperature on slabs obtained by compression moulding. Rectangular samples, with width of 3 mm, thickness of about 4 mm and length of 5 cm

were used. The samples were cut from slabs obtained by using the same conditions adopted for the preparation of films.

7) Analysis UV-Visible Spectrometric

The UV-Visible spectrometry is useful for evaluating the ability of a material to minimize radiation potentially dangerous to the packaged food. The instrument used is a spectrometer Shimadzu UV-2101PC (Shimadzu, Columbia, MD, USA). UV-Vis spectra were recorded in transmission in the range 200–850 nm.

8) Antibacterial Test

The antimicrobial activity of the iPP/ZnOc composites was evaluated using *E. coli* DSM 498T (DSMZ, Braunschweig, Germany) as test microorganisms. The evaluation was performed using the ASTM Standard Test Method E 2149-10 [34]. The preparation of the bacterial inoculum required to grow a fresh 18-h shake culture of *E. coli* DSM 498T in a sterile nutrient broth (LB composition for 1 L: 10 g of triptone, 5 g of yeast extract and 10 g of sodium chloride) The colonies were maintained according to good microbiological practice and examined for purity by creating a streak plate. The bacterial inoculum was diluted using a sterile buffer solution (composition for one litre: 0.150 g of potassium chloride, 2.25 g of sodium chloride, 0.05 g of sodium bicarbonate, 0.12 g of $CaCl_2 \cdot 6H_2O$ and pH = 7) until the solution reached an absorbance of 0.3 ± 0.01 at 600 nm, as measured spectrophotometrically. This solution, which had a concentration of 1.5×10^8–3.0×10^8 colony forming units/mL (CFUs/mL), was diluted with the buffer solution to obtain a final concentration of 1.5×10^6–3×10^6 CFUs/mL, that was the working bacterial dilution.

The experiments were performed in 50 mL sterilized flasks. One gram of the film was maintained in contact with 10 mL of the working bacterial dilution. After 2 min, 100 mL of the working bacterial dilution was transferred to a test tube, which was followed by serial dilution and plating out on Petri dishes (10 mm × 90 mm) in which the culture media was previously poured. The Petri dishes were incubated at 35 °C for 24 h. These dishes represented the T_0 contact time. The flasks were then placed on a wrist-action shaker for 1 h, 24 h, 48 h, 5 days and 10 days. The bacterial concentration in the solutions at these time points was evaluated by again performing serial dilutions and standard plate counting techniques. Three experiments were performed for each composition. The number of colonies in the Petri dish after incubation was converted into the number of colonies that form a unit per millilitre (CFUs/m) of buffer solution in the flask. The percentage reduction (R%) was calculated using the following formula:

$$R\%\,(\mathrm{CFU/mL}) = [(B - A)/B] \times 100, \quad (1)$$

where A = CFUs/mL for the flask containing the sample after the specific contact time and B = CFUs/mL at T_0.

3. Results and Discussion

3.1. Analysis of ZnO and ZnOc Particles

Before blending the ZnOc particles with iPP, an investigation of properties of the ZnO and ZnOc particles has been performed, to assess the amount of stearic acid present on the ZnO particles and the influence of the coating process on the structure, morphology, and thermal stability of the zinc oxide particles. The content of stearic acid present on the surface of the coated particles was evaluated through thermogravimetric analysis. Figure 1 reports the thermogravimetric curves of ZnO and ZnOc particles recorded during the heating rate of 20 °C/min in air from room temperature to 700 °C.

In the entire T range, for ZnO particles, no weight loss was observed. In the case of ZnOc, after the thermal treatment, a weight reduction of about 9% is found. Considering that ZnO does not undergo

degradation, it can be concluded that the weight reduction percentage observed for ZnOc corresponds probably to the percentage of stearic acid present on the surface of the particles.

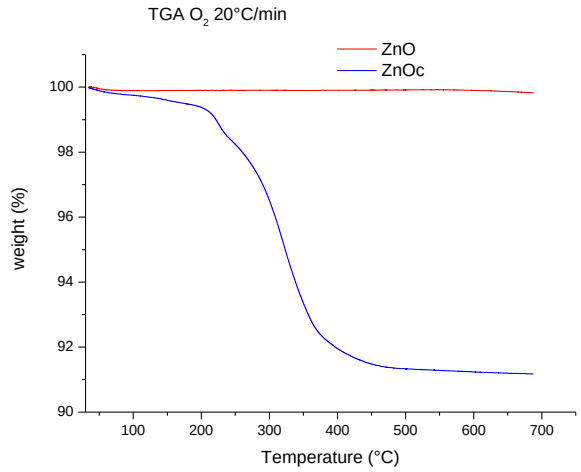

Figure 1. Thermostability curve of ZnO and ZnOc particles.

To study the influence of the stearic acid on the crystalline structure of the ZnO particles, the spectra of X-ray diffraction at high angles were recorded. As shown in Figure 2, the spectrum of the particles of ZnOc presents the same peaks as those of ZnO, suggesting that the coating does not alter the crystalline structure of the particles (zincite) [35].

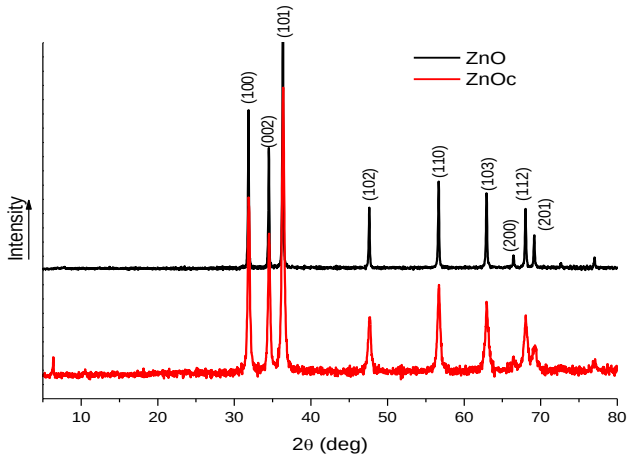

Figure 2. X-ray diffraction pattern of ZnO and ZnOc particles.

In order to recognize the functional groups present, the interaction between the stearic acid and the ZnO particles and to obtain information on the shape of the particles, FTIR analysis was been performed.

Figure 3 reports the FTIR spectrum of ZnOc and ZnO. For the coated sample, different bands can be observed, in particular according to literature [35–38]:

- at 2916 and 2848 cm^{-1}: these vibration bands can be assigned to the "stretching" of the symmetric and asymmetric aliphatic group CH_2;
- at 1460 cm^{-1}: this band is assigned to the vibration of "bending" of aliphatic groups CH_2 and CH_3 of stearic acid;
- at 1540 and 1384 cm^{-1}: these bands are assigned to the asymmetric and symmetric vibrations of the carboxylate group of the stearic acid;

- at around 454 cm^{-1}: These bands give information about the shape of the particles. It is interesting to go deeper into the bands at points 3 and 4.

In particular, the bands at 1540 and 1384 cm^{-1} (region of absorption of the carbonyl C=O) can be related to the coordination behavior of the carboxylate group when it forms complexes with metals. These bands can give important information on the nature of the link between ZnO and the carboxylate group (COO–) of stearic acid.

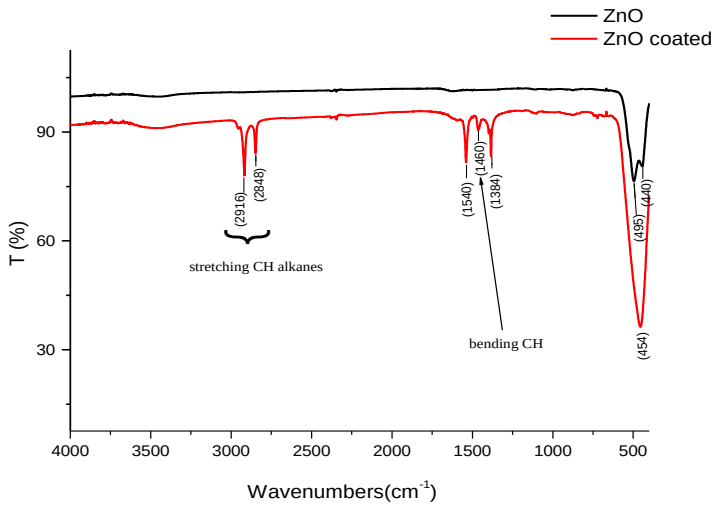

Figure 3. FT-IR spectrum of ZnO and ZnOc powder.

According to literature, the carboxylate group has versatile coordination behavior, when it forms coordination complexes with metals. It can be ionic, monodentate, bidentate chelating or bridging. Measuring the frequency of asymmetric, (ν_{as}(COO–)) and symmetric bands (ν_{as}(COO–) and ν_s(COO–)) and the magnitude of their separation, Δ, (Δ = ν_{as}(COO–) − ν_s(COO–)), the mode of the carboxylate binding with ZnO can be determined [36–38]. Generally, depending on the value of Δ, the following order is proposed for the coordination of carboxylates of divalent metals: Δ(chelating) < Δ(bridge) < Δ(ionic) < Δ(monodentate).

Finally, the assignment of the type of link is done comparing the $\Delta_{(experimental)}$ with that of the corresponding sodium salt ($\Delta_{(sodium\ salt)}$) with the following rules:

- if $\Delta_{(experimental)} \ll \Delta_{(sodium\ salt)}$ is bidentate chelating coordination;
- if $\Delta_{(experimental)} \leqslant \Delta_{(sodium\ salt)}$ is bidentate coordination to bridge;
- if $\Delta_{(experimental)} > \Delta_{(sodium\ salt)}$ coordination is monodentate.

From the figure, $\Delta_{(experimental)}$ = (1540 − 1384) cm^{-1} = 156 cm^{-1}. According to the criterion above, and taking into account that from literature data, the sodium stearate as Δ equal to 138 cm^{-1} [35], it can be concluded that the coordination is monodentate.

The band at 454 cm^{-1} can give information about the shape of the particles. Using the theory of dielectric media [34,36], the single band in ZnOc indicates particles with a spherical shape. It is interesting to make a comparison with the spectrum of the uncoated particles where the two bands indicate the presence of a structure with a mainly prismatic shape.

The morphology of the ZnO and ZnOc particles was studied using scanning electron microscopy (SEM). Figure 4 shows SEM micrographs of ZnO and ZnOc respectively. From the micrographs, it is clear that ZnO particles are characterized by a hexagonal crystal structure, as already emerged from FTIR analysis, with a smooth surface. Moreover, the ZnO particles seem to have a strong tendency to form agglomerates. Contrary ZnOc particles, more homogeneously dispersed in the matrix, have a spherical shape. Comparing the dimensions of the kinds of particles, the size of the ZnO particles ranges between 250 to 500 nm while that of the particles of ZnOc varies between 1 to 1.2 μm.

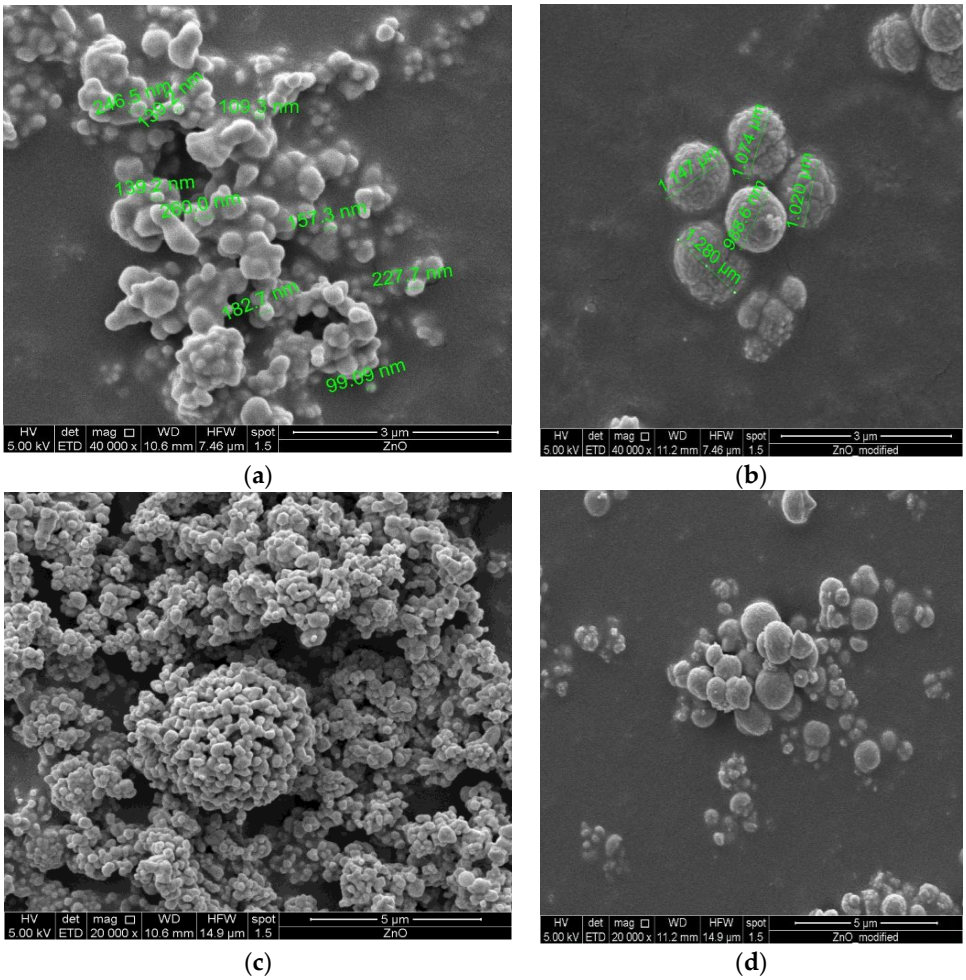

(**a**) (**b**)

(**c**) (**d**)

Figure 4. SEM micrographs of (**a**,**c**) ZnO and (**b**,**d**) ZnOc powders. (a,b) 40000×; (c,d) 20000×.

3.2. *Analysis of the iPP/ZnOc Composites*

3.2.1. Structure and Morphology

The WAXD patterns of iPP and iPP/ZnOc composites are reported in Figure 5. All samples show the presence of the peak at 2θ = 18°–19° characteristic of α form of iPP [39,40]. The sample iPP/5%ZnOc is characterized also by a small percentage of the form β, highlighted by the presence of the peak at 2θ = 16°.

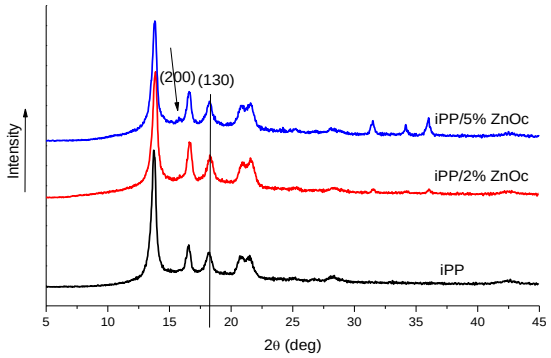

Figure 5. WAXD spectrum of iPP and iPP/ZnOc composites.

UV-Vis spectra are reported in Figure 6. For all samples, an absorption band at 280 nm is observed, probably due to the presence of stabilizer added to commercial iPP. For the samples containing ZnOc, an absorption band is also observed in the region around 385 nm, as indicated by arrows. This band is due to the inherent capacity of the ZnO particles to absorb the UV light [29,30,35,36].

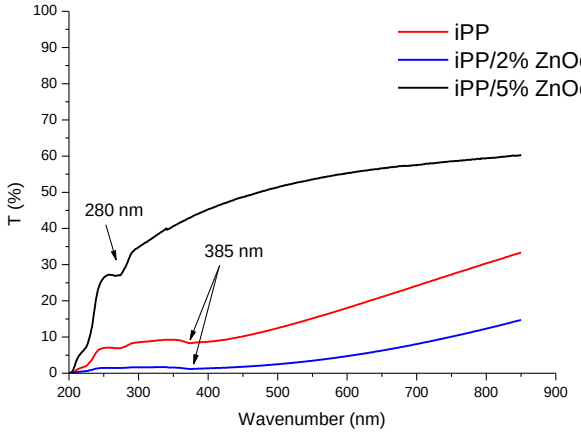

Figure 6. UV-Vis spectrum of iPP and iPP/ZnOc samples.

Figure 7 shows SEM micrographs of the fractured surface of iPP, iPP/2%ZnOc, iPP/5%ZnOc. It is possible to note that the particles are fairly distributed within the polymer matrix. Only a few aggregates with a size of about 5 µm can be observed.

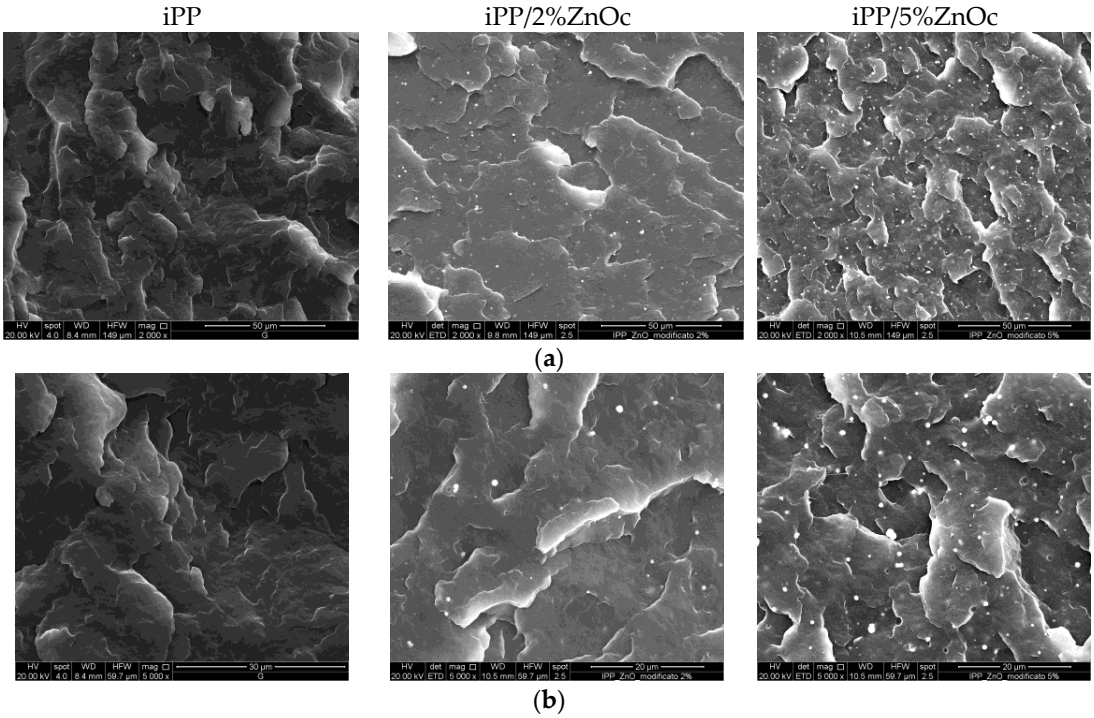

Figure 7. Micrographs of iPP and iPP/ZnOc pellets fractured in liquid nitrogen at magnification (**a**) 2000× and (**b**) 5000×.

Comparing the results with those obtained for the system iPP/ZnO and iPP/PPgMA/ZnO [24] at a given composition, it seems that the coating of the ZnO with stearic acid favors a better dispersion and distribution of the particles in the iPP matrix and prevents the formation of agglomerates.

3.2.2. Thermostability

Figure 8 shows the % weight loss of the samples as function of temperature for iPP and iPP/ZnOc samples, whereas Table 2 reports the values of the temperature at the inflection point of the curve of Figure 8 detected at the maximum of the peak of the first derivative and which corresponds to the maximum rate of the degradation of the sample.

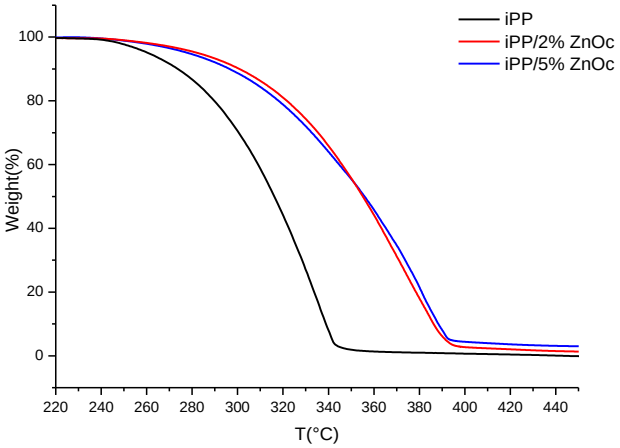

Figure 8. Thermostability curve of iPP and iPP/ZnOc composites.

Table 2. Thermal degradation temperature at which the degradation rate is maximum (T_{max}).

Sample	T_{max} (°C)
iPP	335
iPP/2%ZnOc	375
iPP/5%ZnOc	381

For the two composites, a delay in the temperature of starting degradation, compared to iPP, and a consistent increase of the Tmax are observed. Taking into account that the presence of uncoated ZnO at the same composition did not have consistent influence on the thermostability of iPP, as reported in the paper at reference [22], the increase in thermal stability should be attributed to the stearic acid that coats the ZnO particles. As it was reported in a previous section (see Figure 1), the degradation of the stearic acid starts before the degradation of iPP. The degradation products of the stearic acid probably act as a barrier for the degradation of the matrix also slowing the diffusion of the degradation products of iPP in the sample causing an increase of the thermal stability of the iPP/ZnOc composites.

3.2.3. Mechanical and Impact Properties

Figure 9 shows the stress-strain curves of iPP and iPP/ZnOc composites, whereas Table 3 reports the values of mechanical parameters, (Young modulus (E), stress and strain at the yield point (σ_y, ε_y), and at break (σ_b, ε_b)).

It can be seen that all the samples has the typical behavior of a semi-crystalline polyolefin, with the phenomenon of yield strength, cold drawing, fiber elongation and final break of the fibers.

From the values shown in the Table 3, it can be observed that: (1) the two composite films have similar values of Young modulus and strain at the yield point but higher than those of plain iPP; (2) the elongation at yield and the stress at break point can be considered similar for the three samples (the differences are inside the experimental error), whereas the elongation at break decreases with the addition of ZnOc. Comparing these results with those reported in reference [22], where ZnO not coated was used, it can be observed that the composites with ZnOc present improved mechanical properties.

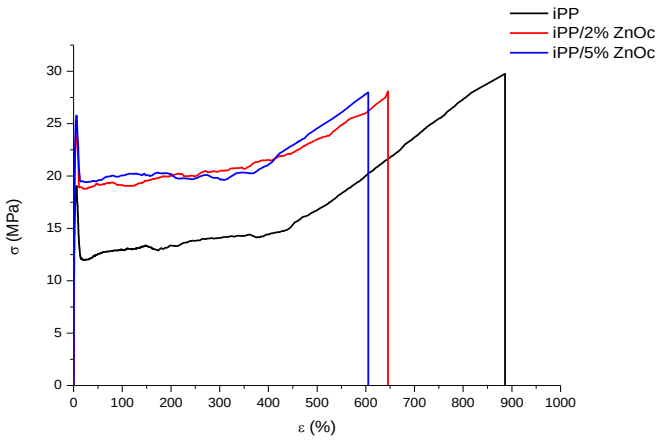

Figure 9. Stress–strain curves of iPP and iPP/ZnOc films.

Table 3. Stress–strain parameters of iPP and iPP/ZnOc composites.

Sample	*E* (MPa)	σ_y (MPa)	ε_y (%)	σ_b (MPa)	ε_b (%)
iPP	1350 ± 100	19 ± 3	7 ± 2	30 ± 3	890 ± 65
iPP/2%ZnOc	1537 ± 44	25 ± 2	7 ± 1	28 ± 4	645 ± 54
iPP/5%ZnOc	1515 ± 79	26 ± 1	7 ± 1	28 ± 3	605 ± 76

Table 4 shows the values of the impact test, in particular the values of the force (F) that the pendulum lost on impact with the sample, the energy (U) absorbed by the samples at the break and the toughness (T). The results demonstrate that the presence of ZnOc increases the toughness; in fact, the toughness of iPP/5%ZnOc sample is 26% higher than that of iPP.

Table 4. Impact tests values for iPP and iPP/ZnOc composites.

Sample	*F* (N)	*E* (J)	*T* (kJ/m^2)
iPP	73 ± 7	0.032 ± 0.008	1.91 ± 0.35
iPP/2%ZnOc	84 ± 3	0.033 ± 0.005	2.07 ± 0.22
iPP/5%ZnOc	89 ± 5	0.042 ± 0.004	2.41 ± 0.14

3.2.4. Antibacterial Properties

In Figure 10, the antimicrobial effect against *E. coli* is presented as a function of time for the different composites. Without ZnO particles, the reference concentration of the micro-organism is measured to be ~2×10^6. After 1 h, no change in the concentration was observed for all samples. By increasing the time, a decrease in the *E. coli* concentration is observed for the composites. The effect is more evident for the iPP/5%ZnOc composite. Significant variations in concentration are observed increasing the contact time and ZnOc content. After 24 h, the concentration of *E. coli* decreases to 8.8×10^5 for iPP/2%ZnOc and 1.7×10^5 for iPP/5%ZnOc. After 48 h, the bacterial concentration was significantly decreased for the iPP/5%ZnOc sample (2×10^3 CFU/mL). The sample iPP/2%ZnOc reaches similar values after five days.

The values of percentage reduction (%R) of *E. coli* for all samples at different contact times are reported in Table 5. Neat iPP exhibits no bactericidal activity, and R was observed to be zero up to day 10. The iPP/5%ZnOc composite exhibited maximum reduction, 99.9%, after 48 h.

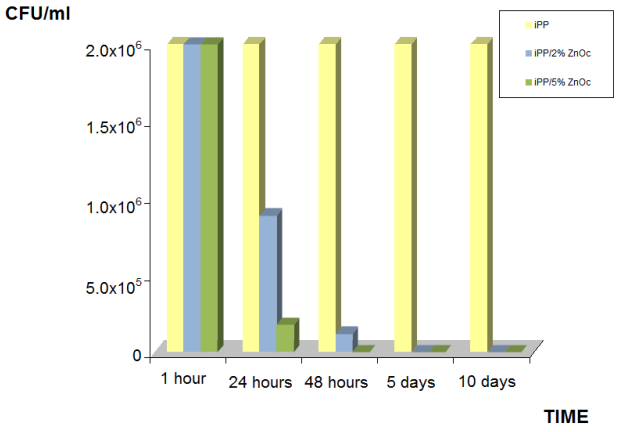

Figure 10. Effect of time and filler content on the antibacterial activity of iPP and iPP/2%–5% ZnOc composites.

Table 5. Percent reduction of *E.coli* at different times of contact with films of iPP and iPP/2%–5% ZnOc.

Sample	%*R* (*t* = 1 h)	%*R* (*t* = 24 h)	%*R* (*t* = 48 h)	%*R* (*t* = 5 days)	%*R* (*t* = 10 days)
iPP	0	0	0	0	0
iPP/2%ZnOc	0	55.61 ± 0.01	94.00 ± 0.01	99.99 ± 0.01	99.99 ± 0.01
iPP/5%ZnOc	0	91.12 ± 0.01	99.99 ± 0.01	99.99 ± 0.01	99.99 ± 0.01

In Table 6 a comparison of the bacterial activity of the three systems, iPP/ZnO, iPP/ZnOc and iPP/PPgMA/ZnO, at the same ZnO content (2%) is reported. From this table, it is clearly confirmed that:

- in the iPP/ZnOc system the ZnOc particles maintain their antibacterial properties against *E. coli*, with respect to the uncoated particles;
- in the system iPP/PPgMA/ZnO, the ZnO particles that are linked to the maleic anhydride groups of PPgMA [24], do not display similar antibacterial activity at least up to 48 h. Probably, the PP chains of the PPgMA, due to the link between MA and ZnO, cover the ZnO particles and hinder the antibacterial activity.

Table 6. Percent reduction of *E. coli* at 48 h and 5 days of contact for iPP and different films at 2% ZnO, (adapted from Table 5 of this paper and references [22,24]).

Sample	%*R* (*t* = 48 h)	%R (*t* = 5 days)
iPP	0	0
iPP/2%ZnO	90	99.99
iPP/2%ZnOc	94	99.99
iPP/$PP_{(9k)}gMA_{(4.8)}$ */2%ZnO	65	NA
iPP/$PP_{(65k)}gMA_{(1.4)}$ **/2%ZnO	60	NA
iPP/$PP_{(95k)}gMA_{(0.5)}$ ***/2%ZnO	31 ± 5	NA

* $PP_{(9k)}gMA_{(4.8)}$ *M*w = 9100 MA (wt %) = 4.8; ** $PP_{(65k)}gMA_{(1.4)}$ *M*w = 65,000 MA (wt %) = 1.4; ***/$PP_{(95k)}gMA_{(0.5)}$ *M*w = 95,000 MA (wt %) = 0.5.

The results obtained from the analysis of antibacterial properties allow us to conclude that the particles of ZnO with stearic acid have relevant antibacterial property against *E. coli*, similar to that of ZnO and that the coating of the particles does not have a negative influence as the coating of the particles with PPgMA [24].

4. Conclusions

This work had as its final objective the preparation of the film based on the isotactic polypropylene matrix intended for packaging food, with improved properties by the addition of ZnO particles coated with stearic acid (ZnOc). The latter has the function of compatibilization between the inorganic metal oxide particles phase and the organic matrix of the isotactic polypropylene. The samples were prepared in a twin-screw extruder and then filmed by a compression molding.

It was observed that the stearic acid coating on the ZnO particles reduces the surface polarity mismatch between iPP and ZnO and allows the formation of a composite with fair distribution of particles.

The principal achievement of the novel composites is the strong antibacterial activity against *E. coli*: the bacterial concentration decreases with increasing concentration of ZnOc and the contact time between the film and the bacterial solution. After 48 h, the bacterial reduction was significantly decreased for the sample containing 5% of ZnOc (R = 99.99%); for the sample iPP/2% ZnOc, it reaches these values after five days.

Moreover, the iPP/ZnOc composites present improvement of the thermal stability, tensile parameters (Young modulus and stress at the yield point) and impact properties with respect to neat iPP, iPP/ZnO, and iPP/PPgMA/ZnO at least for samples containing 2% ZnO [22,24]. It also has to be underlined that the films containing ZnOc show an absorption in the region around 385 nm, confirming that the ZnOc particles also have a shielding effect to UV radiation as those of ZnO as reported in the literature.

On the base of the results obtained, it can be stated that the methodology proposed (using of novel ZnO particles obtained by spray pyrolysis; coating the ZnO with stearic acid and optimization of the processing conditions) is innovative, because no literature is available (at our knowledge) on the properties of such an iPP/ZnOc system prepared directly by melt mixing. Moreover, it is also very efficient in preventing formation of agglomerated domains and in providing a system with improved properties.

In conclusion, the composites iPP/5% ZnOc films have relevant antibacterial property against *E. coli*, higher thermal stability and improved mechanical and impact properties than the pure iPP film so that they are suitable for application in the food industry as active packaging films.

Acknowledgments: The research described herein was partially supported by the European Community's Seventh Framework Programme (ERA-Net Susfood-CEREAL "Improved and resource efficiency throughout the post-harvest chain of fresh-cut fruits and vegetable"), Italian Health Ministry (Progetti Ricerca Corrente/2013 "Impiego di nanopackaging innovativo nella filiera della carne: valutazione dell'efficacia antibatterica e della sicurezza d'uso"), and Italian Ministry of Foreign Affair (Bilateral Project Italy/Quebec 2014–2016 "Sviluppo di nanomateriali ecosostenibili per l'Imballaggio alimentare adatti alla sterilizzazione per radiazione"). Jannette Dexpert-Ghys and Marc Verelst from The Centre d'Élaboration de Matériaux et d'Etudes Structurales (CEMES-CNRS), Toulouse-France, are kindly thanked for supplying ZnO particles obtained by spray-pyrolysis. Ida Romano of the Istituto di Chimica Biomolecolare (CNR), Pozzuoli (NA) Italy is kindly thanked for performing the antimicrobial tests.

Author Contributions: Clara Silvestre and Sossio Cimmino supervised the research program. Clara Silvestre, Sossio Cimmino and Donatella Duraccio designed the setup. Antonella Marra, Valentina Strongone and Donatella Duraccio performed the experiments. All authors contributed to the analysis of the presented experiments and correlation of the different means of investigations. Antonella Marra and Clara Silvestre wrote the initial draft. Clara Silvestre and Sossio Cimmino coordinated the revisions of the draft in the final form.

Conflicts of Interest: The authors declare no conflict of interest.

References

1. Stoimenov, P.K.; Klinger, R.L.; Marchin, G.L.; Klabunde, K.J. Metal oxide nanoparticles as bactericidal agents. *Languimuir* **2002**, *18*, 6679–6686. [CrossRef]
2. Jones, N.; Ray, B.; Ranjit, K.T.; Manna, A.C. Antibacterial activity of ZnO nanoparticle suspensions on a broad spectrum of microorganisms. *FEMS Microbiol. Lett.* **2008**, *279*, 71–76. [CrossRef] [PubMed]

3. Sirelkhatim, A.; Mahmud, S.; Seeni, A.; Kaus, N.H.M.; Ann, L.C.; Bakhori, S.K.M.; Habsah, H.; Dasmawati, M. Review on Zinc oxide nanoparticles: Antibacterial activity and toxicity mechanism. *Nano-Micro Lett.* **2015**, *7*, 219–242. [CrossRef]
4. Padmavathy, N.; Vijayaraghavan, R. Enhanced bioactivity of ZnO nanoparticles—An antimicrobial study. *Sci. Technol. Adv. Mater.* **2008**, *9*. [CrossRef]
5. Yamamoto, O. Influence of particle size on the antibacterial activity of zinc oxide. *Int. J. Inorg. Mater.* **2001**, *3*, 643–646. [CrossRef]
6. Brayner, R.; Ferrari-Iliou, R.; Brivois, N.; Djediat, S.; Benedetti, M.F.; Fiévet, F. Toxicological impact studies based on *Escherichia coli* bacteria in ultrafine ZnO nanoparticles colloidal medium. *Nano Lett.* **2006**, *6*, 866–870. [CrossRef] [PubMed]
7. Zhang, L.; Jiang, Y.; Ding, Y.; Daskalakis, N.; Jeuken, L.; Povey, M.; O'Neill, A.J.; York, D.W. Mechanistic investigation into antibacterial behaviour of suspensions of ZnO nanoparticles against *E. coli*. *J. Nanopart. Res.* **2010**, *12*, 1625–1636. [CrossRef]
8. Li, M.; Zhu, L.; Lin, D. Toxicity of ZnO nanoparticles to *Escherichia coli*: Mechanism and the influence of medium components. *Environ. Sci. Technol.* **2011**, *45*, 1977–1983. [CrossRef] [PubMed]
9. Sawai, J.; Shoji, S.; Igarashi, H.; Hashimoto, A.; Kokugan, T.; Shimizu, M.; Kojima, H. Hydrogen peroxide as an antibacterial factor in zinc oxide powder slurry. *J. Ferment. Bioeng.* **1998**, *86*, 521–522. [CrossRef]
10. Lipovsky, A.; Nitzan, Y.; Gedanken, A.; Lubart, R. Antifungal activity of ZnO nanoparticles—The role of ROS mediated cell injury. *Nanotechnology* **2011**, *22*. [CrossRef] [PubMed]
11. Yamamoto, O.; Sawai, J.; Sasamoto, T. Change in antibacterial characteristics with doping amount of ZnO in MgO-ZnO solid solution. *Int. J. Inorg. Mater.* **2000**, *2*, 451–454. [CrossRef]
12. Silvestre, C.; Duraccio, D.; Cimmino, S. Food packaging based on polymer nanomaterials. *Prog. Polym. Sci.* **2011**, *36*, 1766–1782. [CrossRef]
13. Silvestre, C.; Cimmino, S. *Ecosustainable Polymer Nanomaterials for Food Packaging: Innovative Solutions, Characterization Needs, Safety and Environmental Issues*; Silvestre, C., Cimmino, S., Eds.; CRC Press, Taylor & Francis Group: Boca Raton, FL, USA, 2013.
14. Lagaron, M.; Ocio, M.J.; Lopez-Rubio, A.J. *Antimicrobial Polymers*; Yam, K.L., Lee, D.S., Eds.; John Wiley & Son: Hoboken, NJ, USA, 2012.
15. Matei, A.; Cernica, I.; Cadar, O.; Roman, C.; Schiopu, V. Synthesis and characterization of ZnO—Polymer nanocomposites. *Int. J. Mater. Form.* **2008**, *1*, 767–770. [CrossRef]
16. Huang, C.; Chen, S.; Wei, W.C.J. Processing and property improvement of polymeric composites with added ZnO nanoparticles through microinjection molding. *J. Appl. Polym. Sci.* **2006**, *102*, 6009–6016. [CrossRef]
17. Emamifar, A.; Kadivar, M.; Shahedi, M.; Solimanian-Zad, S. Effect of nanocomposite packaging containing Ag and ZnO on reducing pasteurization temperature of orange juice. *J. Food Process. Preserv.* **2012**, *36*, 104–112. [CrossRef]
18. Droval, G.; Aranberri, I.; Bilbao, A.; German, L.; Verelst, M.; Dexpert-Ghys, J. Antimicrobial activity of nanocomposites: Poly(amide) 6 and low density poly(ethylene) filled with zinc oxide. *E-Polymers* **2008**, *128*, 1–13. [CrossRef]
19. Lepot, N.; van Bael, M.K.; van den Rul, H.; D'Haen, J.; Peeters, R.; Franco, D.; Mullens, J. Influence of incorporation of ZnO nanoparticles and biaxial orientation on mechanical and oxygen barrier properties of polypropylene films for food packaging. *J. Appl. Polym. Sci.* **2015**, *120*, 1616–1623. [CrossRef]
20. Chandramouleeswaran, S.; Mhaske, S.T.; Kathe, A.A.; Varadarajan, P.V.; Prasad, V.; Vigneshwaran, N. Functional behaviour of polypropylene/ZnO-soluble starch nanocomposites. *Nanotechnolohy* **2007**, *18*. [CrossRef]
21. Tang, J.; Wang, Y.; Liu, H.; Belfiore, A. Effects of organic nucleating agents and zinc oxide nanoparticles on isotactic polypropylene crystallization. *Polymer* **2004**, *45*, 2081–2091. [CrossRef]
22. Silvestre, C.; Cimmino, S.; Pezzuto, M.; Marra, A.; Ambrogi, V.; Dexpert-Ghys, J.; Verelst, M.; Augier, S.; Romano, I.; Duraccio, D. Preparation and characterization of isotactic polypropylene/zinc oxide microcomposites with antibacterial activity. *Polym. J.* **2013**, *45*, 938–945. [CrossRef]
23. Duraccio, D.; Silvestre, C.; Pezzuto, M.; Cimmino, S.; Marra, A. Polypropylene and polyethylene-based nanocomposites for food packaging applications. In *Ecosustainable Polymer Nanomaterials for Food Packaging*; Silvestre, C., Cimmino, S., Eds.; CRC Press, Taylor & Francis Group: Boca Raton, FL, USA, 2013; pp. 143–167.

24. Cimmino, S.; Duraccio, D.; Marra, A.; Pezzuto, M.; Romano, I.; Silvestre, C. Effect of compatibilisers on mechanical, barrier and antimicrobial properties of iPP/ZnO nano/microcomposites for food packaging application. *J. Appl. Packag. Res.* **2015**, *7*, 108–127.
25. Erem, A.D.; Ozcan, G.; Skrifvars, M. Antibacterial activity of PA6/ZnO nanocomposite fibers. *Text. Res. J.* **2011**, *81*, 1638–1646. [CrossRef]
26. Murariu, M.; Paint, Y.; Murariu, O.; Raquez, J.M.; Bonnaud, L.; Dubois, P. Current progress in the production of PLA–ZnO nanocomposites: Beneficial effects of chain extender addition on key properties. *J. Appl. Polym. Sci.* **2015**, *132*. [CrossRef]
27. Krunks, M.; Mellikov, E. Zinc oxide thin films by the spray pirolysis method. *Thin Solid Films* **1995**, *270*, 33–36. [CrossRef]
28. Alavi, S.; Caussat, B.; Couderc, J.P.; Dexpert-Ghys, J.; Joffin, N.; Neumeyer, D.; Verelst, M. Spray pyrolysis synthesis of submicronic particles. Possibilities and limits. *Adv. Sci. Technol.* **2003**, *30*, 417–424.
29. Cimmino, S.; Silvestre, C.; Duraccio, D.; Pezzuto, M. Effect of hydrocarbon resin on the morphology and mechanical properties of isotactic polypropylene/clay composites. *J. Appl. Polym. Sci.* **2011**, *119*, 1135–1143. [CrossRef]
30. Kaci, M.; Benhamida, A.; Cimmino, S.; Silvestre, C.; Carfagna, C. Waste and virgin LDPE/PET blends compatibilized with an Ethylene-Butyl Acrylate-Glycidyl Methacrylate (EBAGMA) Terpolymer, 1. *Macromol. Mater. Eng.* **2005**, *290*, 987–995. [CrossRef]
31. Utracki, L.A. Compatibilization of polymer blends. *Can. J. Chem. Eng.* **2002**, *80*, 1008–1016. [CrossRef]
32. Akbar, B.; Bagheri, R. Influence of compatibilizer and processing conditions on morphology, mechanical properties, and deformation mechanism of PP/Clay nanocomposite. *J. Nanomater.* **2012**, *8*. [CrossRef]
33. Bastarrachea, L.J.; Wong, D.E.; Roman, M.J.; Lin, Z.; Goddard, J.M. Active packaging coatings. *Coatings* **2015**, *5*, 771–791. [CrossRef]
34. *ASTM E 2149-10: Standard Test Method for Determining the Antimicrobial Activity of Immobilized Antimicrobial Agents under Dynamic Contact Conditions*; ASTM: West Conshohocken, PA, USA, 2001.
35. Wang, Z.L. Zinc oxide nanostructures: Growth, properties and applications. *J. Phys. Condens. Matter* **2004**, *16*, 829–858. [CrossRef]
36. Zeleňák, V.; Vargová, Z.; Györyová, K. Correletion of infrared spectra of zinc(II) carboxtlates with their structures. *Spectrochim. Acta Part A* **2007**, *66*, 262–272. [CrossRef] [PubMed]
37. Capelle, H.A.; Britcher, L.G.; Morris, G.E. Sodium stearate absorbtion onto titania pigment. *J. Colloid Interface Sci.* **2003**, *268*, 293–300. [CrossRef] [PubMed]
38. Andrés Vergés, M.; Mifsud, A.; Serna, C.J. Formation of rod-like zinc oxide microcrystals in homogeneous solution. *J. Chem. Soc. Farday Trans.* **1990**, *86*, 959–963. [CrossRef]
39. Silvestre, C.; Cimmino, S.; di Pace, E. Morphology of polyolefins. In *Handbook of Polyolefins*, 2nd ed.; Vasile, C., Ed.; Marcel Dekker: New York, NY, USA, 2000; pp. 175–206.
40. Silvestre, C.; Cimmino, S.; Triolo, R. Structure, morphology and crystallization of a random ethylene-propylene copolymer. *J. Polym. Sci. Part B Polym. Phys.* **2003**, *41*, 493–500. [CrossRef]